ELSEVIER

Journal of Fluorine Chemistry 82 (1997) 79–83

JOURNAL OF FLUORINE CHEMISTRY

The decomposition of CF_3OCF_3 to COF_2 and CF_4

J. Pacansky, R.J. Waltman

IBM Almaden Research Center, 650 Harry Road, San Jose, CA, 95120-6099, USA

Received 21 May 1996; accepted 28 July 1996

Abstract

The reaction coordinate for the decomposition of CF_3OCF_3 to COF_2 and CF_4 is computed using Hartree–Fock, MP2, and density functional theories. A transition structure is computed that connects the reactant CF_3OCF_3 to products COF_2 and CF_4. The geometry of the transition structure is characterized, and the energetics for decomposition to COF_2 and CF_4 are compared with simple C–O bond scission. The most reliable results indicate a lower activation energy for decomposition via the transition structure.

Keywords: Polyperfluorinated ethers; Perfluorodimethyl ether; Decomposition reaction; Transition state

1. Introduction

Polyperfluorinated ethers based on homopolymers and/or copolymers of perfluoromethylene oxide $-CF_2O-$, perfluoroethylene oxide $-CF_2CF_2O-$, and perfluoropropylene oxides $-CF(CF_3)CF_2O-$ and $-CF_2CF_2CF_2O-$, serve as important lubricants in a variety of technologies, including computer disks, diffusion pump oils, and high performance turbine jet engines [1–3]. While the physical properties of these materials are intrinsically very stable, they degrade readily under certain environmental conditions, for example, heating in the presence of metal surfaces and Lewis acid sites [4], and irradiation [5]. Experimental data under these conditions indicate that the liquids undergo main chain scission, resulting in mass loss and a change in distribution to lower molecular weight fragments. At the end of the scissioned chains, –CFO end groups are produced and small gas molecules such as COF_2 and CF_4 are evolved. There is a crucial dependence of product distribution on polymer structure and whether or not pendant groups are present. For example, CF_3- pendant groups cause more CF_4 to be produced relative to COF_2 [5].

Perfluorodimethyl ether, CF_3OCF_3 (PFDME), may be considered to be the smallest monomer unit representative of polyperfluorinated ethers. Recent experimental data reveal nearly stoichiometric evolution of COF_2 and CF_4 products on irradiation [6]. In this report we continue our studies on the mechanism(s) of polyperfluoroether degradation. Here, possible reaction coordinates are characterized for the decomposition of CF_3OCF_3 to CF_4 and COF_2 via ab initio computations using Hartree–Fock, MP2, and density functional theories. A transition structure is computed that connects the reactant CF_3OCF_3 to products COF_2 and CF_4. The geometry of the transient structure is characterized, and the energetics for decomposition to COF_2 and CF_4 are compared with simple C–O bond scission. The most reliable results indicate a lower activation energy for decomposition via the transition structure compared with the formation of radical species.

2. Computational method

Ab initio calculations were performed using the Mulliken computer code [7], using IBM RISC 6000 computers. In addition to Hartree–Fock (HF) and Moeller–Plesset second-order perturbation theory (MP2), density functionals using the functional of Perdew and Wang [8], LDFT, and the gradient-corrected functional of Becke, Lee, Yang, and Parr [9], BLYPDFT, were employed. For the open shells, $CF_3\cdot$ and $CF_3O\cdot$, spin restricted wavefunctions were used only at the HF level; spin unrestricted wavefunctions were employed at MP2, LDF, and BLYPDFT, for which the expectation value for the spin eigenfunction S^2 was less than or equal to 0.756 in all cases. All the calculations were performed at the 6-31G* basis set [10]. Harmonic vibrational frequencies were calculated by differentiation of the energy gradient at the optimized geometries. No imaginary frequencies were computed at minima.

3. Results and discussion

The electron beam irradiation of CF_3OCF_3, both in the gas phase and isolated in an argon matrix at low temperatures,

PII S0022-1139(96)03529-4

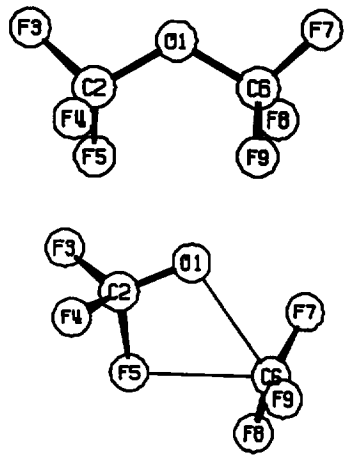

Fig. 1. The HF/6-31G* optimized geometries for PFDME (top) and TS (bottom).

produces COF_2 and CF_4 decomposition products [6]. Hence, the two possible reaction paths that are considered here are a direct C–O bond cleavage (Eq. (1)) followed by a fluorine atom transfer reaction by the radicals, and bond scission reactions via a transition rate (Eq. (2)), in both cases to produce the experimentally observed COF_2 and CF_4 products.

$$CF_3OCF_3 \rightarrow CF_3O\cdot + CF_3\cdot \rightarrow COF_2 + CF_4 \quad (1)$$

$$CF_3OCF_3 \rightarrow TS \rightarrow COF_2 + CF_4 \quad (2)$$

The optimized geometries for CF_3OCF_3 and the transition state structure TS are presented in Fig. 1. The relevant structural parameters are summarized in Tables 1–4. In the reactant PFDME geometry, the F5 and C6 atomic distance is between 2.66 and 2.76 Å, depending on the level of theory employed. At MP2, a distance of 2.692 Å is computed and this value is taken as the best representative distance, under these conditions. The geometry of the transition structure, TS in Fig. 1, is consistent for all of the levels of theory considered here, summarized in Tables 1–4. In every case, the F5–C2–O1–C6 dihedral angle is near 0° (±3°), indicative of planarity within the 'cyclic' transition structure. The scissioning bond O1–C6, computed to be 2.402 Å at HF, is considerably shorter when correlated wavefunctions are employed, 2.058–2.192 Å depending on the level of theory. The other scissioning bond, C2–F5, computed to be 1.468 Å at HF, is appreciably longer at 1.541–1.599 Å, using correlated wavefunctions. The new bond to be formed, F5–C6, computed to be 2.200 Å at HF, is considerably shorter at 1.895–2.024 Å, using correlated wavefunctions. In addition, the O1–C2–F5 bond angle, computed to be 108° at HF, decreases significantly to 102°–103° using correlated wavefunctions. At the transition geometry, the weakening of the C2–F5 and O1–C6 bonds, concomitant with the increased interaction between F5 and C6, causes a fluorine shift F5 to C6, that ultimately produces COF_2 and CF_4.

The relevant bond orders computed at HF/6-31G* are considered in Table 5. At the transition structure, the O1–C2 bond order of 1.503 is 67% larger than the corresponding ether, indicative of a considerable structural shift towards a

Table 1
HF/6-31G* optimized bond distances (Å), angles (deg) and dihedrals (deg)

Parameter	PFDME	TS	COF_2	CF_4
O1–C2	1.356	1.230	1.157	
O1–C6	1.356	2.402		
C2–F3	1.301	1.331	1.290	
C2–F4	1.308	1.331	1.290	
C2–F5	1.310	1.468		
F5–C6	2.695	2.200		1.302
C6–F7	1.301	1.227		1.302
C6–F8	1.308	1.238		1.302
C6–F9	1.310	1.225		1.302
O1–C2–F3	107.09	118.58	125.86	
O1–C2–F4	111.25	118.61	125.86	
O1–C2–F5	111.82	107.70		
O1–C6–F7	107.09	77.70		
O1–C6–F8	111.25	135.30		
O1–C6–F9	111.82	81.99		
C2–O1–C6	121.30	96.95		
C2–F5–C6		98.92		
F5–C6–F7		115.45		109.47
F5–C6–F8		80.59		109.47
F5–C6–F9		96.20		109.47
F7–C6–F8	108.96	115.57		109.47
F7–C6–F9	109.36	121.46		109.47
O1–C2–F3–F4	120.43	136.06	180.00	
C2–F5–C6–F7		−53.68		
F5–C2–O1–C6	−43.47	0.85		
Energy (Hartree)	−747.26551633	−747.09727998	−311.61530618	−435.64520729

Table 2
MP2/6-31G* optimized bond distances (Å), angles (deg) and dihedrals (deg)

Parameter	PFDME	TS	COF_2	CF_4
O1–C2	1.380	1.253	1.186	
O1–C6	1.380	2.110		
C2–F3	1.329	1.348	1.326	
C2–F4	1.337	1.350	1.326	
C2–F5	1.340	1.545		
F5–C6	2.692	1.942		1.329
C6–F7	1.329	1.293		1.329
C6–F8	1.337	1.309		1.329
C6–F9	1.340	1.287		1.329
O1–C2–F3	106.49	119.79	126.24	
O1–C2–F4	111.40	119.82	126.24	
O1–C2–F5	111.96	102.63		
O1–C6–F7	106.49	82.49		
O1–C6–F8	111.40	146.49		
O1–C6–F9	111.96	88.50		
C2–O1–C6	118.18	97.04		
C2–F5–C6		94.87		
F5–C6–F7		126.89		109.47
F5–C6–F8		83.88		109.47
F5–C6–F9		102.56		109.47
F7–C6–F8	109.05	108.09		109.47
F7–C6–F9	109.57	118.31		109.47
O1–C2–F3–F4	120.32	140.26	180.00	
C2–F5–C6–F7		−60.43		
F5–C2–O1–C6	−43.38	3.26		
Energy (Hartree)	−748.70508152	−748.55944408	−312.26516466	−436.46223054

Table 3
LDFT/6-31G* optimized bond distances (Å), angles (deg) and dihedrals (deg)

Parameter	PFDME	TS	COF_2	CF_4
O1–C2	1.373	1.252	1.184	
O1–C6	1.373	2.058		
C2–F3	1.319	1.336	1.315	
C2–F4	1.328	1.334	1.315	
C2–F5	1.331	1.541		
F5–C6	2.661	1.895		1.322
C6–F7	1.319	1.291		1.322
C6–F8	1.328	1.310		1.322
C6–F9	1.331	1.286		1.322
O1–C2–F3	106.72	119.80	126.20	
O1–C2–F4	111.22	119.68	126.20	
O1–C2–F5	111.70	102.35		
O1–C6–F7	106.72	84.10		
O1–C6–F8	111.22	150.33		
O1–C6–F9	111.70	86.80		
C2–O1–C6	117.27	96.52		
C2–F5–C6		94.16		
F5–C6–F7		122.64		109.47
F5–C6–F8		84.19		109.47
F5–C6–F9		108.63		109.47
F7–C6–F8	109.23	107.50		109.47
F7–C6–F9	109.61	118.27		109.47
O1–C2–F3–F4	120.33	140.50	180.00	
C2–F5–C6–F7		−64.61		
F5–C2–O1–C6	−44.44	−2.24		
Energy (Hartree)	−745.52808018	−745.40401532	−310.87850352	−434.62172654

Table 4
BLYPDFT/6-31G* optimized bond distances (Å), angles (deg) and dihedrals (deg)

Parameter	PFDME	TS	COF_2	CF_4
O1–C2	1.400	1.261	1.193	
O1–C6	1.400	2.192		
C2–F3	1.344	1.364	1.342	
C2–F4	1.354	1.364	1.342	
C2–F5	1.356	1.599		
F5–C6	2.764	2.024		1.347
C6–F7	1.344	1.309		1.347
C6–F8	1.354	1.321		1.347
C6–F9	1.356	1.302		1.347
O1–C2–F3	106.19	119.77	126.23	
O1–C2–F4	111.40	119.69	126.23	
O1–C2–F5	112.31	103.39		
O1–C6–F7	106.19	82.74		
O1–C6–F8	111.40	146.07		
O1–C6–F9	112.31	88.17		
C2–O1–C6	118.89	97.75		
C2–F5–C6		94.35		
F5–C6–F7		126.75		109.47
F5–C6–F8		84.04		109.47
F5–C6–F9		102.90		109.47
F7–C6–F8	109.12	108.74		109.47
F7–C6–F9	109.42	117.45		109.47
O1–C2–F3–F4	120.18	140.12	180.00	
C2–F5–C6–F7		−58.31		
F5–C2–O1–C6	−45.63	0.60		
Energy (Hartree)	−750.40842068	−750.29516697	−312.97863339	−437.43255497

Table 5
HF/6-31G* bond orders

Bond	PFDME	TS	COF_2
O1–C2	0.902	1.503	1.985
O1–C6	0.902	0.140	
C2–F3	0.996	0.917	1.019
C2–F4	0.974	0.917	1.019
C2–F5	0.957	0.596	
F5–C6	0.016	0.161	
C6–F7	0.996	1.219	
C6–F8	0.974	1.181	
C6–F9	0.957	1.206	

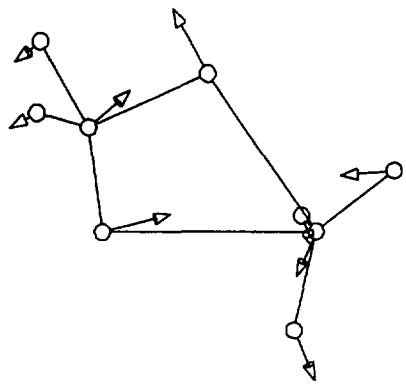

Fig. 2. The HF/6-31G* normal mode displacement vector corresponding to the imaginary frequency computed for the transition structure.

more double-bond-like C=O found in COF_2. Both the O1–C6 and C2–F5 bond orders have decreased considerably in the TS, by almost 85% and 38% respectively, indicative of a considerable weakening of the respective bonds. Concomitantly, the bond order for the forming F5–C6 bond has increased by 906% from the nearly zero 0.016, to the small but significant 0.161. All of these data are indicative that the transition structure will form COF_2 and CF_4.

The transition state structure was further characterized by computing the second derivatives at the optimized geometry. One imaginary frequency was computed: 335i cm^{-1}, 527i cm^{-1}, and 510i cm^{-1}, for HF, LDFT, and BLYPDFT respectively. A plot of the normal coordinate vectors corresponding to the imaginary frequency, Fig. 2, appears to connect reactant (CF_3OCF_3) and product (COF_2, CF_4).

The intramolecular interactions at the transition state are summarized in Table 6 in terms of the computed partial atomic charges. They were obtained from a fit to an electrostatic potential field surrounding the molecule, with a box extension of 2.8 Å from the van der Waals surface, and a step size of 0.3 Å. Relative to CF_3OCF_3, F5 at the transition state is significantly more basic and interacts more strongly with the electropositive C6 carbon atom, Fig. 1. O1 at TS is significantly more negative than the ether CF_3OCF_3, indicative of the availability for bonding. Hence, the O1, C2, F3, and F4 local structure is beginning to resemble COF_2.

Formation of the formal F5–C6 bond concomitant with the scissioning of the O1–C6 and C2–F5 bonds leads to the for-

Table 6
Computed partial atomic charges from an electrostatic potential fit

Atom	PFDME	TS	COF_2	CF_4
HF				
O1	−0.439	−0.793	−0.555	
C2	0.822	0.982	1.036	
F3	−0.191	−0.286	−0.240	
F4	−0.204	−0.287	−0.240	
F5	−0.208	−0.394		−0.201
C6	0.822	0.903		0.802
F7	−0.191	−0.028		−0.201
F8	−0.204	−0.065		−0.201
F9	−0.208	−0.033		−0.201
MP2				
O1	−0.333	−0.565	−0.444	
C2	0.598	0.779	0.844	
F3	−0.135	−0.208	−0.200	
F4	−0.147	−0.212	−0.200	
F5	−0.149	−0.256		−0.152
C6	0.596	0.598		0.610
F7	−0.134	−0.030		−0.152
F8	−0.147	−0.074		−0.152
F9	−0.149	−0.033		−0.152
LDFT				
O1	−0.264	−0.493	−0.419	
C2	0.447	0.654	0.736	
F3	−0.095	−0.168	−0.159	
F4	−0.109	−0.165	−0.159	
F5	−0.112	−0.195		−0.112
C6	0.455	0.440		0.447
F7	−0.098	−0.009		−0.112
F8	−0.111	−0.055		−0.112
F9	−0.114	−0.010		−0.112
BLYPDFT				
O1	−0.276	−0.494	−0.407	
C2	0.491	0.685	0.737	
F3	−0.109	−0.180	−0.165	
F4	−0.121	−0.181	−0.165	
F5	−0.123	−0.246		−0.125
C6	0.491	0.489		0.502
F7	−0.108	−0.014		−0.125
F8	−0.121	−0.043		−0.125
F9	−0.123	−0.016		−0.125

mation of the COF_2 and CF_4 products. As shown in Table 7, the decomposition of CF_3OCF_3 to COF_2 and CF_4 is computed to be exothermic using the higher levels of correlated wavefunctions, MP2 and BLYPDFT. However, the results in Table 7 also indicate that, regardless of the method of calculation, a large activation energy, approximately 70–130 kcal mol^{-1}, separates reactant and product, depending on the reaction path and choice of theory. At the HF level of theory, decomposition via the TS structure is computed to be higher in energy by 26 kcal mol^{-1} than direct bond scission to the $CF_3O\cdot$ and $CF_3\cdot$ radicals. However, energy calculations using the correlated wavefunctions (MP2, DFT) indicate that the transition state TS is actually the lower energy pathway, by 22, 54, and 29 kcal mol^{-1}, for MP2, LDFT, and BLYPDFT respectively.

Table 7
The relative total energies (6-31G*) for the various structures; zero-point energy corrected values are in parentheses

Structure	HF	Relative total energies (kcal mol^{-1})		
		MP2	LDFT	BLYPDFT
Reactant				
CF_3OCF_3	0	0	0	0
Intermediate				
TS(Fig. 1)	105.57 (103.38)	91.39	77.85	71.07 (69.03)
$CF_3O\cdot + CF_3\cdot$	79.94 (75.80)	113.58	131.08	99.61 (96.73)
Product				
$COF_2 + CF_4$	3.14 (0.97)	−14.00	17.48	−1.74 (−3.37)

In summary, the reaction coordinate has been characterized for the decomposition of the model polyperfluorinated ether, CF_3OCF_3, to COF_2 and CF_4. A transition structure has been identified at all levels of theory which facilitates the decomposition to COF_2 and CF_4. When correlated wavefunctions are employed, the reaction path including the transition structure shown in Fig. 1 provides the smaller activation energy to products, compared with a simple initial C–O bond cleavage producing the perfluoromethoxy and perfluoromethyl radicals. One other encouraging feature is the DFT results, in particular, the BLYDFT results, which provide qualitatively a similar reaction coordinate to MP2. For larger systems, this may avoid the computational scaling problems associated with explicit correlation treatment such as MP2 methods, with the possibility of obtaining reliable results. We will continue to evaluate the performance of DFT on perfluorinated ether systems.

References

[1] J.F. Moulder, J.S. Hammond and K.L. Smith, *Appl. Surf. Sci., 25* (1986) 446.
[2] L. Laurenson, N.T.M. Dennis and J. Newton, *Vacuum, 29* (1979) 433.
[3] C.E. Snyder, L.J. Gschwender and C. Tamborski, *Lubr. Eng., 37* (1981) 344.
[4] P.H. Kasai and P. Wheeler, *Appl. Surf. Sci., 52* (1991) 91.
[5] J. Pacansky, R.J. Waltman and C. Wang, *J. Fluorine Chem., 32* (1986) 283.J. Pacansky and R.J. Waltman, *J. Phys. Chem., 95* (1991) 1512.J. Pacansky, R.J. Waltman and M. Maier, *J. Phys. Chem., 91* (1987) 1225.J. Pacansky and R.J. Waltman, *Chem. Mater., 5* (1993) 486.J. Pacansky, R.J. Waltman and G. Pacansky, *Chem. Mater., 5* (1993) 1526.
[6] J. Pacansky, R.J. Waltman and D. Jebens, to be submutted to *J. Phys. Chem.*, 1996.
[7] J.E. Rice, H. Horn, B.H. Lengsfield, A.D. McLean, J.T. Carter, E.S. Replogle, L.A. Barnes, S.A. Maluendes, G.C. Lie, M. Gutowski, W.E. Rudge, Stephan P.A. Sauer, R. Lindh, K. Andersson, T.S. Chevalier, P.-O. Widmark, Djamal Bouzida, G. Pacansky, K. Singh, C.J. Gillan, P. Carnevali, William C. Swope and B. Liu, *Mulliken, version 2.0*, Almaden Research Center, IBM Research Division, 6500 Harry Road, San Jose, CA 95120-6099, 1995.
[8] J.P. Perdew and Y. Wang, *Phys. Rev. B, 45* (1992) 1324.
[9] C. Lee, Y. Wang and R.G. Parr, *Phys. Rev. B, 37* (1988) 785.A.D. Becke, *Phys. Rev. A, 38* (1988) 3098.
[10] K. Raghavachari and J.A. Pople, *Int. J. Quantum Chem., 20* (1981) 1067.